Biochemical and Biophysical Research Communications **267,** 283–289 (2000)
doi:10.1006/bbrc.1999.1967, available online at http://www.idealibrary.com on IDEAL®

Molecular Recognition Templates of Peptides: Driving Force for Molecular Evolution of Peptide Transporters

John W. Payne,[1] Barry M. Grail, and Neil J. Marshall
School of Biological Sciences, University of Wales Bangor, Bangor, Gwynedd LL57 2UW, United Kingdom

Received November 29, 1999

Small peptides derived from protein hydrolysis occur ubiquitously. To utilize these structurally diverse compounds, organisms possess generic peptide transporters for di- (Dpp), tri- (Tpp), and oligopeptides (Opp). Using conformational analysis, we describe the predominant conformers of di-, tri-, and oligopeptides in water; dipeptides occur as nine main groups, defined by specific combinations of torsional angles. The molecular recognition templates (MRTs) of substrates for Dpp and Tpp comprise distinct groups of dipeptide conformers plus folded tripeptide conformers with matching spatial distribution of recognition features; for Opp, the MRT involves specific oligopeptide conformers with extended backbones. For any peptide, the proportion of its conformers in a particular MRT correlates with its relative binding and transport by each transporter. Thus, peptide transporters have evolved complementary specificities to optimize utilization of the universal peptide pool. The general applicability of MRTs should facilitate rational design and targeting of peptide-based prodrugs.

Small peptides, composed of two to five protein amino acid residues, exist in 3.3684×10^6 different sequences. Furthermore, they are flexible molecules and each exists in aqueous solution as a mixture of interconverting conformers, making the structural variety present in this repertoire of compounds enormous. They comprise a universal source of unrivalled nutrients, and peptide transporters occur in all organisms to transfer these polar molecules across membranes [1–5]. Here, we address the problem of molecular recognition faced by these transporters in optimizing their ability to handle all components of this peptide pool. The essential features of substrate specificity of peptide transporters have been determined from transport studies and ligand binding assays and are common in all organisms. Substrates optimally need a free, protonated N-terminal α-amino group; a free, C-terminal carboxylate; all L-stereochemistry and a trans peptide bond; in short, features shared by all peptides [1–7]. Some modifications to the basic structural features can be tolerated, which makes peptide transporters attractive targets for delivery of therapeutic peptidomimetic drugs [3, 5–9]. *Escherichia coli* and *Salmonella typhimurium* possess three archetypal peptide transporters: the ABC transporters Dpp and Opp [2, 6, 10–12], and Tpp, which is energized by a proton motive force [2, 6]. Similarly, studies of mammalian di- and tripeptide uptake in the intestine showed it contains (at least) two systems for these substrates, but longer peptides are not absorbed [1, 4, 5, 13]. PepT1 and PepT2, analogous to Dpp/Tpp, have been characterized in mammalian intestine and kidney and are single protein transporters energized by a proton gradient [5, 14, 15]. X-ray crystal structures of the periplasmic peptide-binding proteins DppA and OppA with bound ligands, have revealed how the charged termini are stabilized, and side chains accommodated in cavities containing variable water molecules [7, 16, 18–20]. However, even with all this detailed information, it has still not been possible to explain why some peptides are good substrates and others are poor, making it difficult to predict affinities and to design peptide mimetics that can exploit peptide transporters for their delivery and bioactivity.

MATERIALS AND METHODS

Peptide uptake assays. Transport of peptides was measured using fluorescence and radioactive techniques [2, 6] with peptide transport mutants described previously [6]. The relative abilities of peptides to compete for uptake with toxic peptides, e.g., GV was measured from their capacities to decrease the sizes of inhibition zones around GV in a modified agar plate assay (unpublished). A membrane filtration assay was used to measure ligand binding to OppA and DppA as described [6].

Conformational analyses of peptides. Peptides were modeled using SYBYL 6.2 and 6.4 (Tripos Inc., St. Louis, MO). Preformed amino acid fragments were joined to construct molecules with the required sequence and chirality, and charges were assigned. Default SYBYL atom types were generally applied except for protonated amino

[1] To whom correspondence should be addressed. Fax: 44 (0) 1248 370731. E-mail: j.w.payne@bangor.ac.uk.

0006-291X/00 $35.00

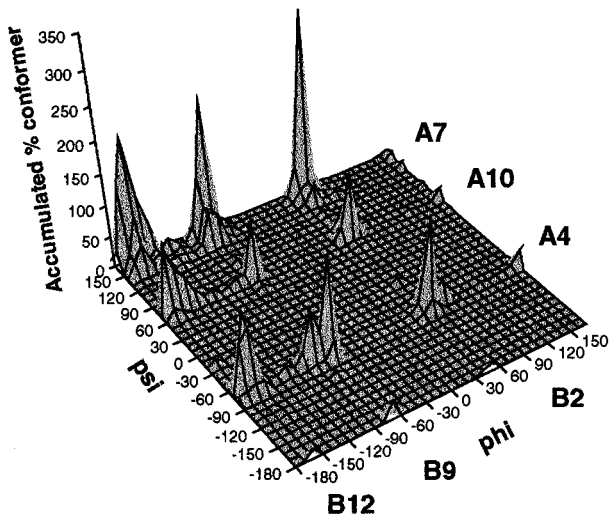

FIG. 1. 3D pseudo-Ramachandran plot for dipeptides. For each dipeptide, conformers were identified by random search. Psi, ψ and phi, ϕ space around the peptide bond was divided into 10° sectors, and the distribution of specific torsional angles for each conformer was plotted against its percentage of the total conformers. Graph shows the result of aggregating all such data for all conformers for fifty dipeptides. Psi, ψ and phi, ϕ axes are divided into 30° sectors designated A1–A12 and B1–B12, respectively.

groups and carboxylate oxygens, which were assigned N.4 and O.co2 atom types, respectively. Minimized starting structures, with trans ω bonds, were submitted to Random Search for between 1K and 50K iterations, with all rotatable bonds free to be searched; on occasions, results for several independent searches on a peptide were combined. Unique conformers were distinguished using an RMS threshold of 0.2 A with chirality checking and an absolute energy cutoff of 70 kcal/mol. Each conformer was minimized using the Powell method with gradient termination, and its energy calculated using Tripos force field and Pullman charges. Implicit aqueous solvation was applied using a distance-based dielectric function with a constant of 80. Conformers were displayed in SYBYL molecular spreadsheet format where calculations of Boltzmann distribution, percentage contribution and measurements of: N–C distance, ψ^1, ψ^2 (TOR2, TOR6), ω^1, ω^2 (TOR3, TOR7), ϕ^1, ϕ^2 (TOR4, TOR8) and other torsional angles were carried out. For each individual peptide, ψ and ϕ angles were divided into thirty six 10° sectors, and ω torsions were categorized as *cis* or *trans;* the percentage contributions of conformers within each ψ, ω, ϕ combination were summed. Data accumulated from all related peptides, e.g., dipeptides, were combined and the overall percentage contribution in all ψ, ω, ϕ combinations calculated. To classify the resultant nine sets of conformer structures, ψ, ϕ conformational space was divided into twelve 30° sectors designated A1 to A12 and B1 to B12, respectively, and each class was described by reference to its principal location within this grid, e.g., A7B9. Distribution of N–C distance for each group of related peptides, e.g., tripeptides, was determined by first dividing the maximum N–C distance found into 0.5 A bins; for each individual peptide its percentage of conformers in each bin was calculated and this procedure was repeated for all related peptides to give their aggregated distribution of N–C distances.

RESULTS

Our premise in this work was that common structural patterns must occur amongst peptides that provide the basis for specific substrate recognition by each transporter. Thus, we sought to define the molecular recognition template (MRT) for natural substrates of each transporter using the following features: (i) presence of charged N-terminal α-amino and C-terminal α-carboxyl groups, allowing electrostatic and hydrogen-bond donor or acceptor properties; (ii) sets of torsional angles (ψ, ϕ, and ω) in the backbone; (iii) stereochemistry of α-carbon chiral centers; (iv) N–C distance between terminal amino-N and carboxylate-C atoms; (v) chi (χ) space torsional angles of side chains;

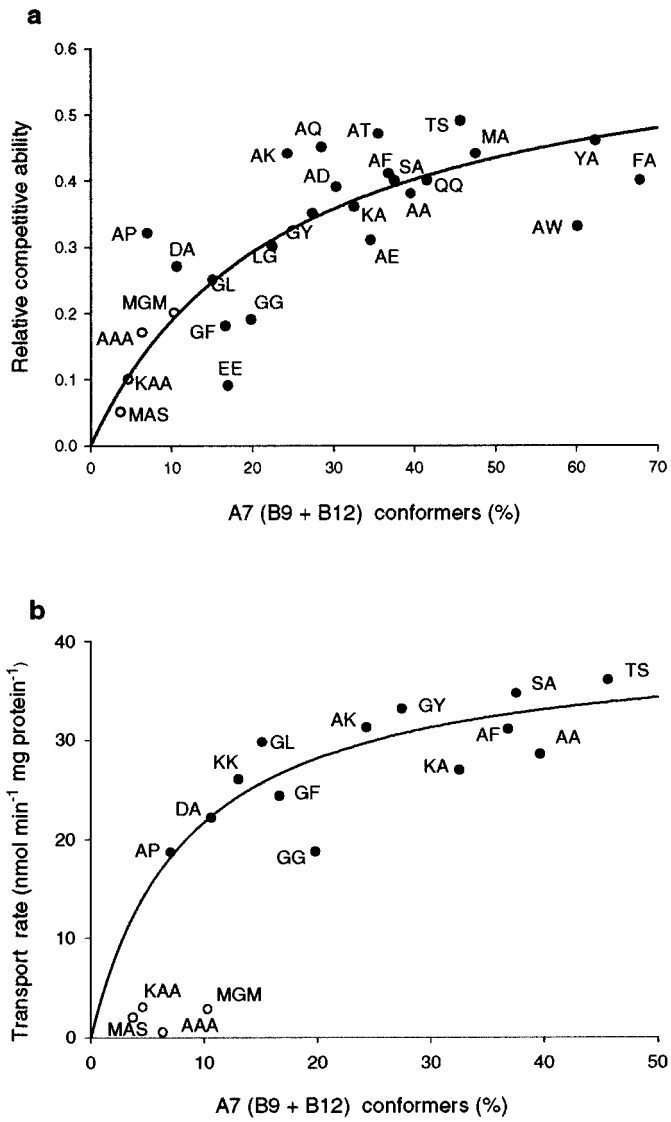

FIG. 2. Relationship between amount of peptide conformers in A7(B9 + B12) conformations and (a) relative competitive abilities of peptides in overcoming inhibition arising from uptake of VG by Dpp and (b) peptide transport by Dpp. The transport mutant PA0410 (dpp^+, opp^-, tpp^-) [6] of *E. coli* K12, which is sensitive to valine, was used. Amino acid residues are abbreviated using single letter code; tripeptides (○) and dipeptides (●). For tripeptide conformers, an additional screen of N–C distance of 4.5–6.0 A was applied to identify folded conformers.

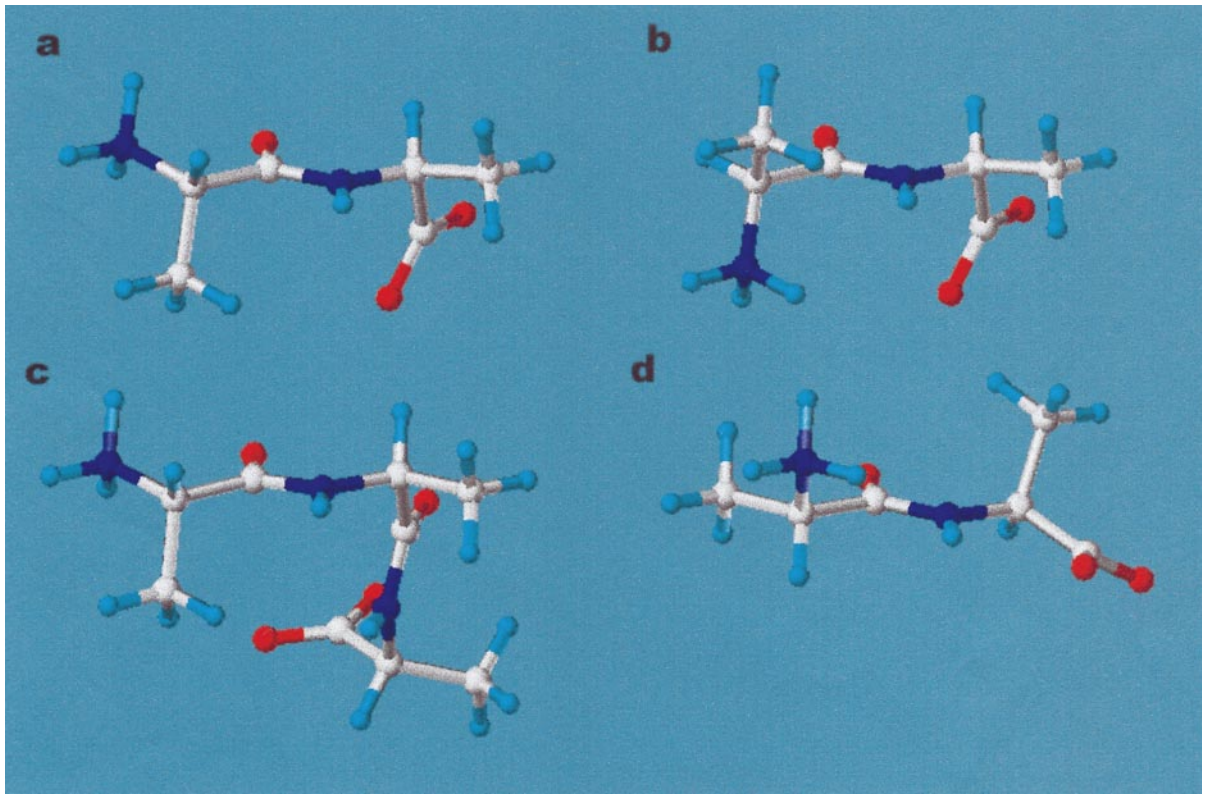

FIG. 3. Ball and stick representations of model peptides AA and AAA, illustrating psi (ψ) (TOR2), omega (ω) (TOR3) and phi (ϕ) (TOR4) torsions for di- and tripeptide conformers that define the molecular recognition templates of Dpp (A7(B9 + B12)) and Tpp (A4,A10(B9 + B12)). For AAA, the appropriate folded forms are identified by including N–C distances required for substrates of Dpp and Tpp. All MRT forms can be generated by combining appropriate (ψ) and (ϕ) torsions; for illustration, the following specific conformers are shown: (a) AA in A7B9; (b) AA in A10B9; (c) AAA in folded A7 form; and (d) AA in A4B12.

(vi) hydrogen-bond donor and acceptor properties of peptide bond atoms; (vii) charge fields around N-terminal α-amino group and C-terminal α-carboxyl group. To satisfy important features above: (i) only peptides with charged N- and C-termini were modeled, (ii) only trans ω bonds were considered, and (iii) all L-residues were used. Conformational analyses of over fifty di- and fifty oligopeptides were performed. For each peptide a collection of conformers resulted, which were ranked by energy, and the percentage contribution of each calculated using Boltzmann distribution. For every conformer present at $>0.1\%$, psi (ψ) and phi (ϕ) space was divided into 10° sectors. The distribution of torsional angles for all conformers was computed in SYBYL spreadsheet and plotted on a 3D pseudo-Ramachandran plot (3DPR), relating ψ, ϕ and percent conformer.

MRTs for dipeptides. A collection of dipeptides was first analyzed, selected as representative of a range of side chains and also as being available for experimental studies. The result of aggregating the data for all conformers for fifty dipeptides is shown in Fig. 1. Dipeptides adopt a limited set of nine combinations of ψ and ϕ; for ψ, -50 to $-85°$; $+140$ to $-175°$; and $+50$ to $+85°$, designated A4, A7, and A10, respectively; and for ϕ, $+40$ to $+85°$; -95 to $-50°$; and -130 to $+175°$, designated B2, B9, and B12, respectively. If peptides with G or P are excluded, these angular ranges become considerably tighter. Conformers were screened so as to exclude any in which side chains occupied unacceptable χ^2 based upon the crystal structure of liganded DppA and structural correlations found here (see below). In most cases, little or no correction was needed, but with bulky or charged side chains some conformers were disallowed. For any peptide, its percentage of conformers in each form, e.g., A7B9 can be calculated.

These sets of conformational types were related to substrate specificities determined experimentally for Dpp and Tpp. For these studies, mutants possessing only one peptide transporter were produced in *Escherichia coli* K12 [6], a strain that is sensitive to valine [2]. For studying Dpp, twenty three dipeptides were assayed as competitors for uptake of the toxic dipeptide VG (Fig. 2a) and 13 measured as transport substrates (Fig. 2b). The peptides were then ranked in order of effectiveness and related to the calculated subsets of psi and phi conformers populated by these dipeptides. A correlation was found with only one subset, A7(B9 +

B12) (Fig. 3); there was no significant correlation with occupation of any other of the combinations of psi and phi angles. Endorsement of these conclusions also came from results of ligand-binding assays with DppA [2, 6] (see below). These identified relationships between unique conformers and biological activity of Dpp were corroborated independently by the reported crystal structure of GL bound to DppA [16], in which GL occurs as an A7B9 conformer with an N–C distance of 5.6 A (see below). The conformers predicted as the MRT of Dpp have their peptide bond N and O atoms orientated so that H-bonding with protein backbone atoms in DppA is optimized, and side chains are directed so as to occupy appropriate cavities [16]. For Tpp, competitive ability to protect against the inhibition resulting from uptake of VG (Fig. 4a) and direct assays of substrate transport (Fig. 4b) were determined in an *E. coli* mutant strain PA0333 lacking Dpp and Opp activities [6]. These relative activities were related to all subsets of conformers and found to correlate only with the sum of A4(B9 + B12) plus A10(B9 + B12) conformers, a result that indicates the torsional specificities of the MRT for Tpp. Most dipeptides possess a majority of their conformers in both MRT recognition types, A7(B9 + B12) or A4,A10(B9 + B12) (Fig. 1), making them good substrates for both Dpp and Tpp, whereas some, e.g., YA, FA (<10% Tpp conformers), exist predominately in one or other type making them rather specific for only one system, a feature already noted in transport studies [2]. For any particular peptide, its lowest energy conformers may not be substrates for either transporter, a situation that is understandable when such peptides are seen as being only individual components of a larger peptide pool. Dipeptides with G and/or P residues have the bulk of their conformers with torsional angles at the extreme limits of the ranges defined by A7B9 etc. and, consequently, are expected to be poor substrates for both systems, although we have not moderated the percent conformers for GG in Fig. 2 to reflect their lower effectiveness; in support of this conclusion, GG is found to be especially poorly recognized by peptide transporters in all tested species [1, 2, 4].

MRTs for tripeptides. Tripeptides are also transported by both Dpp and Tpp although less well than dipeptides, making their true substrates the combined di-, tripeptide pool (8.4×10^3 compounds). Thus, MRTs of these transporters need to embrace conformational features shared by both peptide groups. Therefore, amongst tripeptide conformers it may be expected that ones exist with appropriate ψ and ϕ angles, and, to achieve involvement of the critical charged termini, with N–C distance geometries matching those for dipeptide substrates. To identify these tripeptide forms, fifteen sets of dipeptide conformers were first analyzed for N–C distances and their overall distribution is shown in Fig. 5. The range for (A7(B9 + B12)) substrates of Dpp was 4.5–6.0 A and for (A4,A10(B9 + B12)) substrates of Tpp was 4.0–5.5 A. A set of fourteen tripeptides, which were selected in part because of their availability for experimental study, was subjected to conformational analysis, and the distribution of N–C distances for their complement of conformers is shown in Fig. 5. Screening these conformers for ones with A7(B9,B12) plus an N–C distance of 4.5–6.0 A identified a subset of matching "folded" structures as

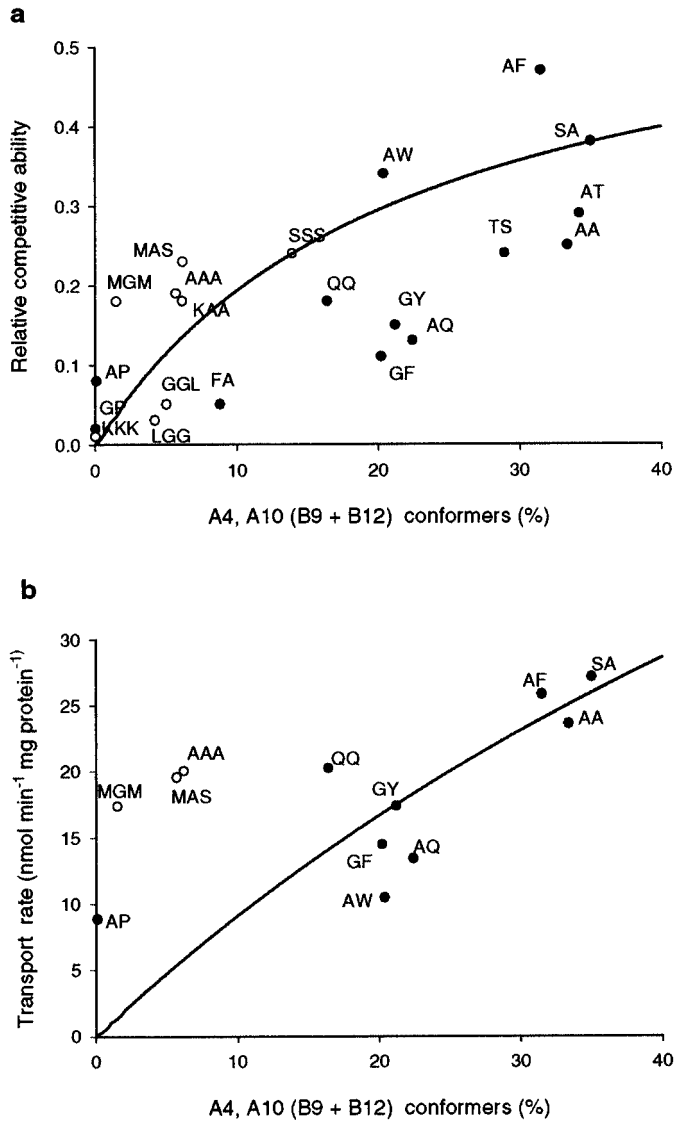

FIG. 4. Relationship between amount of peptide conformers in A4,A10(B9 + B12) conformations and (a) relative competitive abilities of peptides in overcoming inhibition arising from uptake of VG by Tpp and (b) peptide transport by Tpp. The transport mutant PA0333 (*dpp*$^-$, *opp*$^-$, *tpp*$^+$) [6] of *E. coli* K12, which is sensitive to valine, was used. Amino acid residues are abbreviated using single-letter code; tripeptides (○) and dipeptides (●). For tripeptide conformers, an additional screen of N–C distance of 4.5–5.5 A was applied to identify folded conformers.

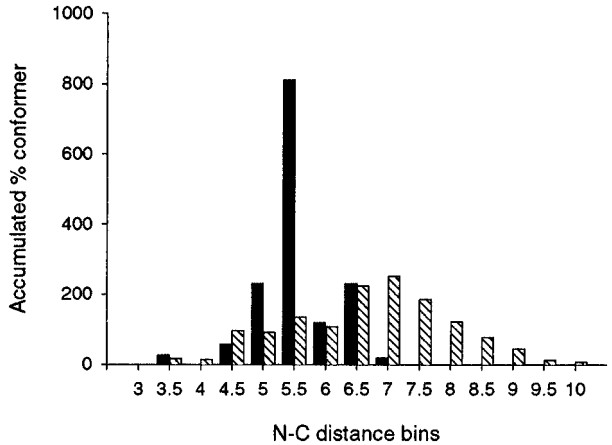

FIG. 5. N–C distance distribution for di- and tripeptide conformers. All conformers were included so that the shortest N–C values correspond to peptides containing cis peptide bonds. Dipeptides are filled bars and tripeptides are cross-hatched. Bin distances are labeled such that e.g., maximum distribution for dipeptides occurs in range >5.0–≤5.5 A.

putative Dpp substrates (Fig. 3), and using the parameters for Tpp (A4,A10(B9 + B12)) with an N–C distance of 4.0–5.5 A a further subset was identified. For these folded conformers, atom-based superimposition procedures and often even simple visual inspection, showed they effectively matched the dipeptide-derived MRTs at the critical N- and C-termini, and the first peptide unit (ψ, ϕ, and ω) and side chain; the second peptide bond and C-terminal side chain effectively formed a structural unit orientated similarly to the C-terminal side chain of dipeptides allowing it to fit into the relevant pocket of transporter proteins. These folded forms generally comprised just a few percent of total conformers. For Dpp, the percentage of relevant folded conformers of four tripeptides was related to results for their transport and to their competitive effects on uptake of inhibitory VG, and good correlations were obtained (Fig. 2); this conclusion was endorsed by measurements of tripeptide binding to DppA (see below). Similarly, for Tpp a good correlation was found for the folded tripeptide conformers identified as putative substrates when these were related to transport rates and to competition with VG (Fig. 4). The ability to plot both di- and tripeptides together reflects the fact that together they comprise the substrates for these transporters. In accord with experiments showing that only di- and tripeptides are substrates [1, 2, 4, 6], analogous modeling of tetra- and higher peptides indicated that they cannot adopt folded conformations able to match adequately the MRTs of Dpp or Tpp.

Oligopeptide transporters. Opp transports oligopeptides, and to a lesser extent dipeptides. Crystal structures of liganded-OppA show analogous mechanisms of binding as for DppA, with charged termini stabilized through interaction with oppositely-charged protein residues, side chains accommodated in cavities with associated water molecules, and backbone peptide bond atoms hydrogen bonded to the protein [18–20]. A collection of over fifty peptides with three to five residues was modeled to try to identify an MRT for oligopeptide transporters. Individual conformers were analyzed as above, and for each peptide bond in turn percentages of conformers with their associated ψ, ϕ angles were aggregated and plotted on separate 3DPR (results not shown); N–C distances for each conformer were also measured. For tripeptides, an N-terminal ψ of A7 combined with a ϕ of B9 predominates, with A7B12 present in lesser amounts; N–C distances distribute biphasically, with those around 5.5 A corresponding to the above "folded" structures and ones >6.5 A representing "extended" forms (Fig. 5). With higher oligomers, a ψ of A7 becomes relatively more dominant. By analogy with the correlation of particular di-, and tripeptide conformers to the MRTs of Dpp and Tpp, we extracted for each oligopeptide its percentage of conformers with A7B9 torsions and N–C distance >6.5 A; subsequent ψ, ϕ angles (TOR6, 8, etc.) are variable but combinations of appropriate ones can for the present purpose be conveniently subsumed into N–C distances.

Transport specificity for Dpp and Opp is conferred by DppA and OppA, respectively [2, 6]. Thus, for these transporters, substrate specificity can be measured using radioactive-ligand binding assays with purified binding proteins [6]. For DppA, the results for di- and tripeptide binding correlated only with the content of conformers in the A7(B9 + B12)-dependent MRT described above (Fig. 6a). Similarly, for OppA, the relative binding values for eight tripeptides obtained using competition for binding of [$^{125}I_2$]YGG, only correlated with the percentage conformer for each peptide present as A7,B9 with N–C distance >6.5 A (Fig. 6b). GGG with very few relevant conformers is the worst competitor/substrate of OppA, and in separate experiments is found to be the least well transported by Opp; other peptides have relative transport rates in accord with their content of relevant conformers (results not shown). These conclusions relating modeling predictions for oligopeptides to their binding and transport properties by Opp, find complete support in the crystal structures of liganded OppA, which show that oligopeptides adopt what is essentially an "extended" A7B9 conformation [18–20].

DISCUSSION

Universal nature of peptide MRTs. Most studies on computing peptide structures have considered them as components of proteins, modeling them with acylated N- and amidated C-termini and usually with the aim of obtaining precise conformational descriptions of specific, low energy conformers [21–23]. Several computa-

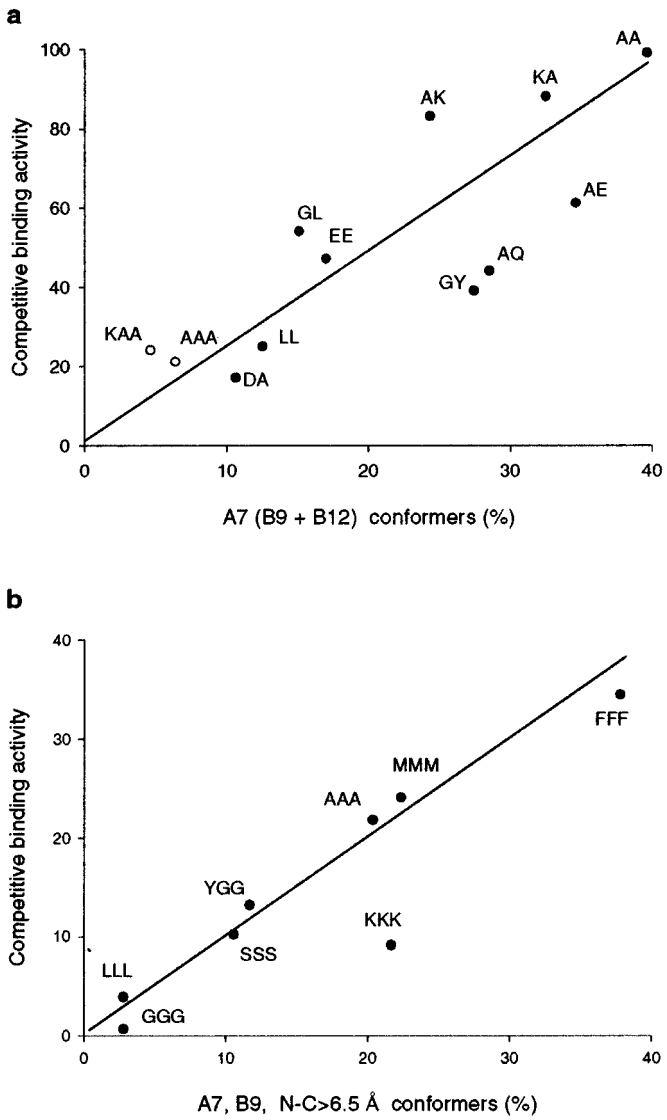

FIG. 6. Relationships between amounts of specific conformers and peptide binding (a) to DppA and (b) to OppA. (a) Relative abilities of various peptides to compete with G-[^{125}I]Y for binding to DppA [6]; values are compared with AA, which was set to 100. (b) With OppA, [$^{125}I_2$]-YGG was used as substrate with tripeptides as competitors [6]. Results are expressed as relative competitive values derived from experiments using several competitor: substrate ratios.

tional approaches have been used e.g., *ab initio,* molecular mechanics, molecular dynamics etc, employing varied techniques, e.g., grid search, explicit solvation, distance-dependent dielectric constant, etc. There have been few computational analyses of simple, charged peptides [24]. Our objectives here in searching for common MRTs amongst collections of peptides are different from the above and limit the computational options. For example, modeling incorporating explicit water molecules is not computationally sensible, but importantly, when we applied it to AA (results not shown) and analyzed the resultant collection of conformers, the results did not differ significantly from those obtained using our chosen protocol. Our approach allowed identification of structural features shared by peptides that appear to provide the driving force for the molecular evolution of the complementary substrate specificities of a universal group of peptide transporters. Features that define the MRT can be considered as influencing the effectiveness of substrate recognition and binding in two ways. Firstly, each feature influences the conformer repertoire in solution upon which recognition depends, and secondly, each is required for consolidating interactions with the transporter that ensures specificity and affinity. For peptides, binding/transport ability is mainly determined by the proportion of conformers that exist in the relevant MRT. Conformers exist in a dynamic equilibrium in which the relative amounts of each class of conformer remain effectively constant under fixed conditions. The "effective concentration" of a substrate can be considered as its chemical concentration multiplied by its percent MRT. This conclusion is essentially an alternative way of stating a central tenet of structure-based ligand design, that for a flexible ligand its binding affinity will be improved if its conformational motion can be restricted to that of the ligand-bound form. The need to consider ligand conformations when attempting to explain relative peptide binding has been mentioned in discussions of thermodynamic results for peptide binding to OppA [20], which show enthalpy-entropy compensation [20, 25]. It seems that similar situations may apply to the substrate specificities of peptidases and some other enzymes. A corollary of the present results is that for particular peptides with unique bioactivities e.g., enkephalins, the MRTs for their receptors are likely to occur amongst those high energy, least abundant conformers that are structurally distinct from the MRTs described here, endowing them with unique substrate specificity and affinity.

Testing the results of modeling against biological specificity gave comparable conclusions with various binding and transport assays for Dpp and Opp, and allowed their MRTs to be identified and iteratively refined; these structural correlations were independently validated by the finding that peptide ligands adopt these conformations in crystal structures of liganded DppA and OppA. Thus, by analogy, the predicted MRT for Tpp, which is a membrane protein for which no crystal structure is available, can be assumed to be correct with equal confidence. It seems probable that these MRTs for bacterial peptide transporters are applicable generally, because all will have evolved similarly to recognize components of the universal peptide pool. Thus, *E. coli* is a good model for mammalian transporters and vice versa, a view supported by extensive measurements in bacteria [1, 2], and on intestinal peptide transport [4, 5, 13]. Other attempts to model specificity of intestinal transporters have not

provided adequate descriptions of the molecular recognition features described here [3, 26, 27].

Knowledge of the MRTs for peptide transporters should permit rational design of bioactive mimetics able to exploit such systems, e.g., targeting of antimicrobial agents, enhanced oral and renal absorption of therapeutic drugs, plant growth regulators and herbicides, and insecticides. Initial studies to test this approach, modeling naturally occurring antimicrobial prodrugs [8, 9] and various therapeutic, peptidomimetic compounds e.g., ACE inhibitors, penicillins, and cephalosporins support this expectation (unpublished results).

ACKNOWLEDGMENTS

We thank G. M. Payne, M. W. Smith, D. R. Tyreman, S. Gupta, and H. L. Jones for their help with various aspects of this study and the Biotechnology and Biological Sciences Research Council and the Research and Development Committee of the North West Wales NHS Trust for funding parts of the work.

REFERENCES

1. Matthews, D. M., and Payne, J. W. (1980) *Curr. Top. Membr. Transp.* **14,** 331–425.
2. Payne, J. W., and Smith, M. W. (1994) *Adv. Microbial Physiol.* **36,** 1–80.
3. Taylor, M. D., and Amidon, G. L. (1995) *in* Peptide-Based Drug Design: Controlling Transport and Metabolism, Am. Chem. Soc., Washington, DC.
4. Matthews, D. M. (1991) *in* Protein Absorption: Development and Present State of the Subject, Wiley-Liss, New York.
5. Fei, Y. J., Ganapathy, V., and Leibach, F. H. (1998) *Prog. Nucleic Acid Res. Mol. Biol.* **58,** 239–261.
6. Smith, M. W., Tyreman, D. R., Payne, G. M., Marshall, N. J., and Payne, J. W. (1999) *Microbiology* **145,** 2891–2901.
7. Wilkinson, A. J. (1996) *Chem. Biol.* **3,** 519–524.
8. Payne, J. W. (1995) *in* Peptide-Based Drug Design: Controlling Transport and Metabolism. (Taylor, M. D., and. Amidon, G. L., Eds.), pp. 341–367, Am. Chem. Soc., Washington, DC.
9. Tyreman, D. R., *et al.* (1998) *in* Peptides in Mammalian Protein Metabolism: Tissue Utilization and Clinical Targeting (Grimble, G. K., and Backwell, F. R. C., Eds.), pp. 141–157, Portland Press, London.
10. Abouhamad, W. N., Manson, M., Gibson, M. M., and Higgins, C. F. (1991) *Mol. Microbiol.* **5,** 1035–1047.
11. Hiles, I. D., Gallagher, M. P., Jamieson, D. J., and Higgins, C. F. (1987) *J. Mol. Biol.* **195,** 125–142.
12. Olson, E. R., Dunyak, D. S., Jurss, L. M., and Poorman, R. A. (1991) *J. Bacteriol.* **173,** 234–244.
13. Ganapathy, V., Brandsch, M., and Leibach, F. H. (1994) *in* Physiology of the Gastrointestinal Tract (Johnson, L. R., Ed.), 3rd ed., pp. 1773–1794, Raven Press, New York.
14. Liang, R., *et al.* (1995) *J. Biol. Chem.* **270,** 6456–6463.
15. Liu, W., *et al.* (1995) *Biochim. Biophys. Acta* **1235,** 461–466.
16. Dunten, P. W., and Mowbray, S. L. (1995) *Protein Sci.* **4,** 2327–2334.
17. Nickitenko, A. V., Trakhanov, S., and Quiocho, F. (1995) *Biochemistry* **34,** 16585–16595.
18. Tame, J. R. H., Dodson, E. J., Murshudov, G. N., Higgins, C. F., and Wilkinson, A. J. (1995) *Structure* **3,** 1395–1406.
19. Sleigh, S. H., Tame, J. R. H., Dodson, E. J., and Wilkinson, A. J. (1997) *Biochemistry* **36,** 9747–9758.
20. Davies, G. D., Hubbard, R. E., and Tame, J. R. H. (1999) *Protein Sci.* **8,** 1–13.
21. Cornell, W. D., Caldwell, J. W., and Kollman, P. A. (1997) *J. Chem. Phys.* **94,** 1417–1435.
22. Nikiforovich, G. V. (1994) *Int. J. Pept. Protein Res.* **44,** 513–531.
23. Marshall, G. R., Beusen, D. D., and Nikiforovich, G. V. (1993) *in* Peptides: Chemistry, Structure and Biology. Proceedings of the 13th American Peptide Symposium (Hodges, R. S., and Smith, J. A., Eds.), pp. 1105–1117.
24. Knapp-Mohammady, M., Jalkanen, K. J., Nardi, F., Wade, R. C., and Suhai, S. (1999) *Chem. Phys.* **240,** 63–77.
25. Klebe, G., and Bohm, H. J. (1997) *J. Recept. Signal Transduct. Res.* **17,** 459–473.
26. Li, J., and Hidalgo, I. J. (1996) *J. Drug Target.* **4,** 9–17.
27. Swaan, P. W., and Tukker, J. J. (1997) *J. Pharm. Sci.* **86,** 596–602.